JACS
JOURNAL OF THE AMERICAN CHEMICAL SOCIETY
Communication
pubs.acs.org/JACS

Atomic Details of the Interactions of Glycosaminoglycans with Amyloid-β Fibrils

Katie L. Stewart,[†] Eleri Hughes,[‡] Edwin A. Yates,[§] Geoffrey R. Akien,[‡] Teng-Yi Huang,[⊥] Marcelo A. Lima,[∥] Timothy R. Rudd,[#] Marco Guerrini,[▽] Shang-Cheng Hung,*[,§] Sheena E. Radford,*[,†] and David A. Middleton*[,‡]

[†]Astbury Centre for Structural Molecular Biology, School of Molecular and Cellular Biology, University of Leeds, Leeds LS2 9JT, United Kingdom

[‡]Department of Chemistry, University of Lancaster, Lancaster LA1 4YB, United Kingdom

[§]Department of Biochemistry, Institute of Integrative Biology, University of Liverpool, Liverpool L69 7ZB, United Kingdom

[⊥]Genomics Research Center, Academia Sinica, No. 128, Section 2, Academia Road, Taipei 115, Taiwan

[∥]Department of Biochemistry, Federal University of Sao Paulo, Rua Três de Maio, São Paulo 40440-020, Brazil

[#]National Institute of Biological Standards and Control, South Mimms, Potters Bar, Hertfordshire EN6 3QC, United Kingdom

[▽]Ronzoni Institute for Chemical and Biochemical Research, Via G. Colombo 81, Milano 20133 Italy

Supporting Information

ABSTRACT: The amyloid plaques associated with Alzheimer's disease (AD) comprise fibrillar amyloid-β (Aβ) peptides as well as non-protein factors including glycosaminoglycan (GAG) polysaccharides. GAGs affect the kinetics and pathway of Aβ self-assembly and can impede fibril clearance; thus, they may be accessory molecules in AD. Here we report the first high-resolution details of GAG−Aβ fibril interactions from the perspective of the saccharide. Binding analysis indicated that the GAG proxy heparin has a remarkably high affinity for Aβ fibrils with 3-fold cross-sectional symmetry (3Q). Chemical synthesis of a uniformly ^{13}C-labeled octasaccharide heparin analogue enabled magic-angle spinning solid-state NMR of the GAG bound to 3Q fibrils, and measurements of dynamics revealed a tight complex in which all saccharide residues are restrained without undergoing substantial conformational changes. Intramolecular ^{13}C−^{15}N dipolar dephasing is consistent with close (<5 Å) contact between GAG anomeric position(s) and one or more histidine residues in the fibrils. These data provide a detailed model for the interaction between 3Q-seeded Aβ40 fibrils and a major non-protein component of AD plaques, and they reveal that GAG−amyloid interactions display a range of affinities that critically depend on the precise details of the fibril architecture.

Alzheimer's disease (AD) is characterized pathologically by an accumulation of insoluble plaques within the extracellular spaces of brain tissue. The main protein constituents of AD plaques are the 40- and 42-residue amyloid-β peptides, Aβ40 and Aβ42, derived from the amyloid precursor protein. The relationship between Aβ self-assembly and disease has not been elucidated, but the development of drugs that lower the propensity of Aβ peptides to self-assemble or reduce the aggregate concentration is a therapeutic goal.[1] Aβ amyloid plaques in the brain are highly heterogeneous, comprising fibrous proteins of different structural organizations,[2] metal ions, nucleic acids, and glycosaminoglycans (GAGs),[3] the linear sulfated polysaccharide components of proteoglycans. GAGs accelerate Aβ polymerization[4] and increase fibril resistance to proteolytic degradation.[5] The recent clinical failure of drugs that inhibit Aβ aggregation *in vitro*[6] may reflect, in part, the role of molecules such as GAGs in the development and stabilization of amyloid in the brain. Work focusing on GAGs has revealed a complicated picture of interactions with protein networks, with low binding specificity and high redundancy among heterogeneous saccharide units.[7]

We previously detected a GAG binding site at the surface of fibrillar MAβ40 (an Aβ40 homologue with an N-terminal methionine) from heparin-induced peptide chemical shift perturbations measured using cross-polarization magic-angle spinning (CP-MAS) solid-state NMR (SSNMR).[8] In this and previous studies, heparin was employed as a proxy for the highly sulfated domain of heparan sulfate (HS) commonly associated with amyloid plaques and sharing the same disaccharide units as heparin.[9] Aβ40 fibrils are polymorphic, and fibril strains having approximately 2-fold (2A) or 3-fold (3Q) cross-sectional symmetry can be selected by seeding and morphologically confirmed by SSNMR.[8,10] Previously, we developed an assay to quantify heparin binding which involves sedimentation of bound heparin with fibrils and quantifies unbound heparin by addition of heparinase enzyme, creating a spectroscopically active product.[8] We found that heparin binds with surprisingly higher affinity to MAβ40 3Q fibrils than to MAβ40 2A fibrils, and the SSNMR data suggest that heparin recognizes the junctions of the triangular cross-section that is unique in the structures of 3Q fibrils (Figure S1).[8]

Here we show, in addition, that *de novo* MAβ40 fibrils assembled without seeding, a peptide comprised of Aβ residues 16−22 (KLVFFAE), human amylin (hIAPP) which is 47% similar

Received: March 17, 2016
Published: June 9, 2016

DOI: 10.1021/jacs.6b02816
J. Am. Chem. Soc. 2016, 138, 8328−8331

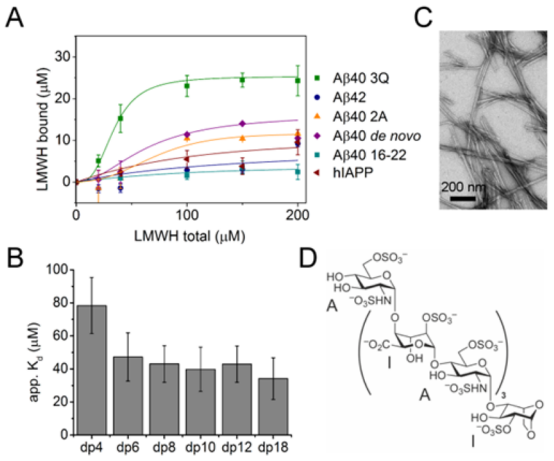

Figure 1. GAG binding to amyloid fibrils. (A) Binding affinities of fibrils to low-molecular-weight heparin (LMWH, dp16). Curves were obtained by nonlinear least-squares fitting of a Hill function. (B) Apparent dissociation constants K_d for MAβ40 3Q fibrils binding heparin fragments of different degrees of polymerization (dp4−dp18). (C) TEM image of 3Q fibrils co-sedimented with [U-^{13}C]OHA. (D) Chemical structure of [U-^{13}C]OHA.

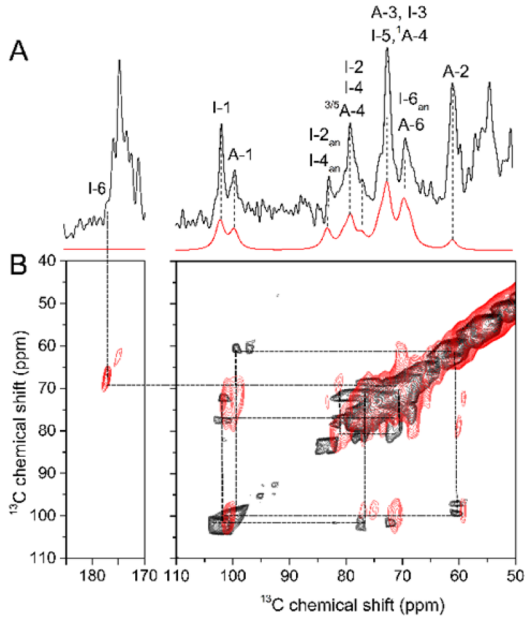

Figure 2. ^{13}C CP-MAS SSNMR spectra of the [U-^{15}N] 3Q fibril−[U-^{13}C]OHA complex. (A) Experimental spectrum (black) at 4 °C, with assignments, and a simulated spectrum from the solution chemical shifts (red). (B) 2D symmetrized ^{13}C−^{13}C spectrum recorded with a DARR mixing time of 20 ms (black) and an unsymmetrized spectrum at 50 ms mixing time (red).

in sequence to Aβ40, and a uniform morphology of MAβ42 fibrils[11] bind weakly to low-molecular-weight heparin (LMWH) (Figures 1A and S2). These binding differences suggest a unique relationship between 3Q fibrils in particular and heparin, but the origin of this specific relationship requires a full molecular-level understanding of the 3Q fibril−heparin interaction. Whether all heparin residues lie in contact with specific amino acids (Figure S1, top), or whether part of heparin lies away from the fibril surface (Figure S1, bottom), is not known. Here, synthesis of a uniformly ^{13}C-labeled octasaccharide heparin analogue ([U-^{13}C]OHA) has enabled the detailed analysis of a GAG−amyloid interaction for the first time from the GAG perspective, using CP-MAS SSNMR to observe the GAG bound to insoluble 3Q MAβ40 fibrils.

We assessed the affinities of heparin-derived polysaccharides of different length (dp4−dp18) for 3Q-seeded MAβ40 fibrils, using the GAG binding assay described above and in ref 8. All heparin fragments show saturable binding, consistent with specific GAG−fibril interactions, and an apparent $B_{max} < 20\ \mu$M (Figures S3 and S4). Heparin tetrasaccharide (dp4) shows the lowest binding affinity ($K_d = 78 \pm 17\ \mu$M), and although the larger fragments show slight increases in binding affinity, there is no significant difference between the K_d values for dp6−dp18 (Figures 1B and S3). An octasaccharide (dp8; $K_d = 43 \pm 11\ \mu$M) was thus chosen as a representative GAG to investigate amyloid binding in structural detail. [U-^{13}C]OHA (synthesized as in ref 12) consists of alternating 1−4-linked, 6-O-sulfated, N-sulfated α-D-glucosamine [amino sugar (A)], and 2-O-sulfated α-L-iduronic acid (I) units, with a 1,6-anhydro ether bridge in the terminal iduronate ring (Figure 1D) maintaining a closed ring at the former reducing terminus. A 2-fold molar excess of [U-^{13}C]OHA was added to ^{15}N-labeled MAβ40 fibrils prepared by seeding with the 3Q morphology.[10] ^{13}C spectra of [U-^{13}C]-labeled seeded fibrils resembled previously published MAβ40 3Q spectra,[8] verifying the fibril morphology. Transmission electron microscopy (TEM) confirms that the linear unbranched fibrils are maintained (Figure 1C). The fibrils were isolated by centrifugation, and the pellet, estimated to contain 600 nmol of MAβ40 and 170 nmol of bound [U-^{13}C]OHA, was analyzed by ^{13}C CP-MAS SSNMR, revealing signature peaks (60−102 ppm) from the octasaccharide. Under CP-MAS, signals are detected only from nuclei in environments where molecular dynamics are too slow (<10^4 Hz) to average the ^{1}H−^{13}C dipolar couplings (e.g., ref 14). Hence, the observed [U-^{13}C]OHA peaks must arise from octasaccharide associated with the insoluble fibrils. Although the peaks are too broad to resolve residue-specific detail, a two-dimensional ^{13}C−^{13}C SSNMR spectrum (Figure 2B) and tentative peak assignments from a HSQC solution spectrum (Figure S5) enabled resonances to be attributed to positions on the glucosamine and iduronate residues. The changes in chemical shifts upon binding are small (Table S1), which argues against major conformational perturbations that can result in significant changes in chemical shifts, particularly if hydrogen bonding is disrupted.[13]

The bound saccharide dynamics were assessed further by CP-MAS NMR. A ^{13}C refocused INEPT[15] SSNMR spectrum at 4 °C, which detects only long-lifetime coherences from highly mobile groups, is dominated by peaks from MAβ40 (12−68 ppm), with very weak signals from 68 to 78 ppm that may arise from a small mobile fraction of bound or unbound [U-^{13}C]OHA. The absence of peaks around 100 ppm from A-1 and I-1 implies that large-scale motional fluctuations, involving the entire octasaccharide backbone, do not occur. Measurements of motionally sensitive cross-polarization rates R_{HC} and rotating frame relaxation rates $R_{1\rho H}$ for the CH groups at 4 °C (Figure 3B; original data in Figure S6) are typical of organic solids with restricted molecular dynamics.[16] The rates remain essentially the same at −25 °C, which suggests that the saccharide dynamics are similarly impaired in the frozen and non-frozen states. Increased dynamics from −25 to 4 °C (including faster rates of chemical exchange between free and bound states) would result in slower cross-polarization and relaxation rates (see SI and Figure S7 for further discussion).[17] Order parameters S_{CH} determined from octasaccharide ^{13}C−^{1}H dipolar couplings (Figure S8) are near the rigid-limit value of 1.0 and consistent with low-amplitude motions of ring C−H bonds

DOI: 10.1021/jacs.6b02816
J. Am. Chem. Soc. 2016, 138, 8328−8331

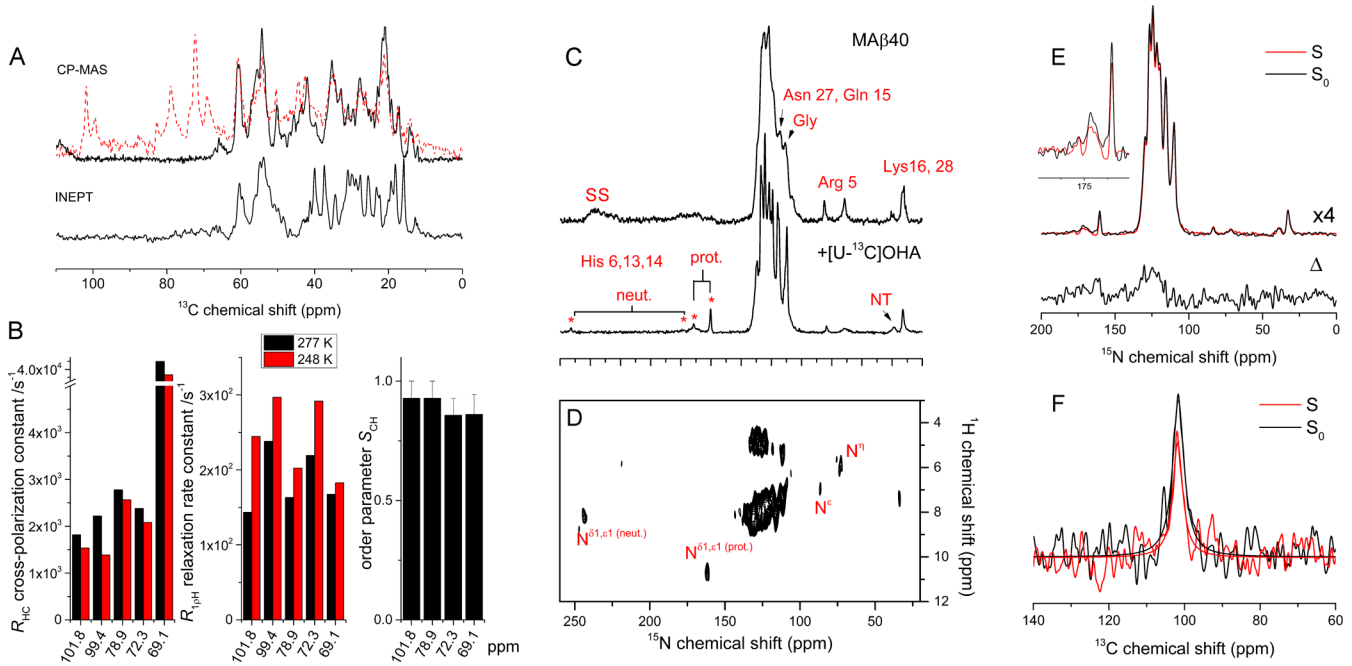

Figure 3. SSNMR analysis of [U-^{13}C]OHA interactions with [U-^{15}N]MAβ40 fibrils. (A) CP-MAS spectrum of fibrils alone (top), overlaid with the spectrum from Figure 2A (red) and a refocused INEPT spectrum of the complex of fibrils and [U-^{13}C]OHA (bottom). (B) Cross-polarization rate constants R_{HC} and proton rotating frame relaxation rates $R_{1\rho H}$ of [U-^{13}C]OHA bound to the fibrils. (C) ^{15}N CP-MAS spectra of fibrils alone (top) and with [U-^{13}C]OHA (bottom). Neut = neutral; prot. = protonated; SS = spinning sideband; NT = N-terminal amine. (D) ^{1}H−^{15}N HETCOR spectrum. (E,F) Measurements of dipolar couplings between fibrils and [U-^{13}C]OHA at −25 °C. (E) Full-echo (S_0) and dephased-echo (S) ^{15}N{^{13}C} REDOR spectra (8.3 ms dephasing) and difference (Δ). (F) ^{13}C{^{15}N} FSR spectra (6.4 ms dephasing) obtained with selective refocusing applied at the frequencies of $^{15}N^{\delta1/\varepsilon2}$ and C-1 of [U-^{13}C]OHA (red) and a full-echo spectrum (black).

on the sub-millisecond time scale. These data strongly suggest that all octasaccharide residues are restrained by intimate contact with MAβ40.

We next sought to identify close contacts between [U-^{15}N]-MAβ40 fibrils and [U-^{13}C]OHA. The ^{15}N CP-MAS spectrum of 3Q fibrils alone shows sharp peaks from Arg and Lys side chains and His $^{15}N^{\delta1/\varepsilon2}$ resonances (160−180 ppm) that are much broader, possibly due to proton exchange or tautomerization.[11] The ^{15}N 1D and ^{1}H−^{15}N HETCOR spectra of the [U-^{13}C]OHA−fibril complex reveal the appearance of a new sharp peak at ∼161 ppm (Figure 3C,D) and several sharper peaks assigned to backbone and Asn/Gln amides, which suggest a general ordering of the fibrils in the presence of the GAG, and a new sharp peak at ∼161 ppm attributed to His $N^{\varepsilon2}$. Histidine $^{15}N^{\varepsilon2}$ and $^{15}N^{\delta1}$ chemical shifts for model tripeptides are 173−176 ppm for the acidic form (and $^{1}H^{\varepsilon2}/^{1}H^{\delta1}$ shifts are >10 ppm) and ∼231 and 181 ppm for the conjugate base.[18] Here the peak at 161 ppm may reflect the stabilization of protonated His ring(s) by the octasaccharide CO_2^- and SO_3^- groups. A non-selective ^{15}N-observed, ^{13}C-dephased rotational-echo double-resonance (^{15}N-{^{13}C}REDOR) experiment (Figure 3E) showed weak dephasing of peptide amide resonances (112−130 ppm) and possibly also of His resonances, although the signal-to-noise ratio is rather poor. Dipolar dephasing of resonances assigned to Arg, Lys, and Gly was not observed above the noise. Dephasing was not quantified because of uncertainties arising from there being a 3-fold excess of fibrils over [U-^{13}C]OHA and because of small contributions from ^{13}C at natural abundance. A ^{13}C-observed frequency-selective rotational-echo double-resonance (FSR) experiment[19] was used to detect specific ^{15}N−^{13}C dipolar interactions between His side-group $^{15}N^{\delta1/\varepsilon2}$ sites and saccharide C-1 carbons in the 97−100 ppm region. The observed dipolar dephasing ($S/S_0 = 0.72 \pm 0.15$) corresponds to a ^{13}C−^{15}N distance of 3.1−4.6 Å for a single spin pair, consistent with His−[U-^{13}C]OHA interactions. The SSNMR measurements provide new clues about the selectivity of heparin-derived GAGs for MAβ40 fibrils with 3Q morphology and highlight the role of saccharide interactions with histidines (H6, H13, and/or H14) in the formation of the GAG−3Q fibril complex. We confirmed that GAG sulfate moieties are critically important for this interaction by showing that fully desulfated heparin does not bind to the fibrils (Figure S9A). GAG sulfate groups may thus interact with H6 and H13 if the GAG recognizes the junctions of the unique triangular cross-section of the 3Q morphology, whereas interactions with H14 would require binding to the outer surface common to both 2A and 3Q morphologies (Figures S10 and S11). The higher affinity of heparin for 3Q than for 2A fibrils favors the preferential recognition of the unique junctions of 3Q. A 3Q-seeded variant of MAβ40, H6F, shows reduced heparin binding ($K_d = 100 \pm 14$ μM, compared to 43 μM for dp8, Figures S9B and S10), which implies that H6 is involved in, although not essential for, complex formation. [U-^{13}C]OHA may bind tightly if its anionic groups are oriented approximately parallel to the fibril long axis, allowing interactions with polycationic ladders of residues from the repeating peptide units. Computational molecular docking of OHA in the cleft at the triangular junctions, restrained by a distance of <4.0 Å between $N^{\delta1/\varepsilon2}$ sites of appropriate H6 rings in the flexible N-terminal region and octasaccharide C-1 positions, allows for ionic interactions between sulfate and imdazo groups of H6 and H13 on opposite faces (Figure 4A), as well as hydrogen bonding with N27 (which previously showed >1 ppm chemical shift perturbations upon heparin binding[8]), acting in concert to strengthen the interaction between peptide and saccharide further. The presence of Asn residues alongside cationic residues

DOI: 10.1021/jacs.6b02816
J. Am. Chem. Soc. 2016, 138, 8328−8331

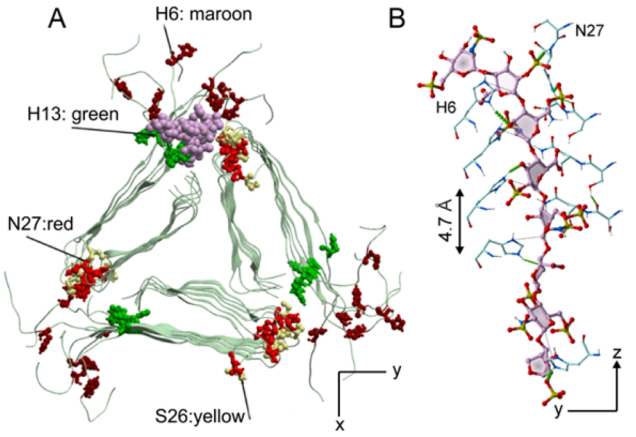

Figure 4. Model of [U-^{13}C]OHA binding to MAβ40 fibrils. (A) Cross-sectional view of the 3Q fibril, from PDB structure 2lmq (negative stagger, with nine flexible N-terminal residues added), viewed down the fibril axis (z) and highlighting key binding residues and OHA (purple spheres) docked in one of the three cleft sites. (B) View of an octasaccharide molecule with repeating H6 and N27 residues.

has been posited recently as a characteristic of GAG binding sites in proteins.[20] The octasaccharide in a broadly linear conformation bears O- and N-linked SO_3^- groups that match approximately the periodicity of repeating side groups (~4.7 Å) (Figure 4B). This, and our binding data on other fibril types (Figure 1A), suggest that GAG−3Q interactions are more specific than mere electrostatic patterning. Instead, the structure of the 3Q fibril corners localizes multiple charged and hydrogen-bonding residues in a favorable orientation, providing a tight and specific binding site for heparin (Figure S11). The involvement of histidine residues in this interaction suggests that disease states manifesting local pH changes could enhance GAG−fibril interactions, leading to altered rates of disease progression. Fibrils with different binding modes and affinities may rationalize the array of phenotypes that are present in AD and the range of time scales over which the disease progresses.

The work presented provides the first glimpse of a GAG chain binding tightly and offers rationalization for the quantifiable and surprisingly specific affinity for a well-defined morphology of Aβ40 fibrils. A 3-fold conformation of Aβ has been isolated and purified from human brain tissue, underscoring the relevance of this structural motif in disease.[2] These results reveal that while GAGs are commonly found associated with amyloid plaques, GAG−fibril interactions show remarkable specificity, which may influence the varied properties of amyloid fibrils in disease.

■ ASSOCIATED CONTENT

Supporting Information

The Supporting Information is available free of charge on the ACS Publications website at DOI: 10.1021/jacs.6b02816.

Additional information as noted in the text, including Figures S1−S11 and Table S1, and details of all preparative and experimental methods (PDF)

■ AUTHOR INFORMATION

Corresponding Authors

*schung@gate.sinica.edu.tw
*s.e.radford@leeds.ac.uk
*d.middleton@lancaster.ac.uk

Notes

The authors declare no competing financial interest.

■ ACKNOWLEDGMENTS

The BBSRC (UK) is thanked for grants BB/K01451X/1 and BB/K015958/1. Academia Sinica and Ministry of Science and Technology also provided funding (MOST 104-0210-01-09-02 and 104-2628-M-001-001). We thank Dr R. Tycko for providing the fibril seeds and Dr. G. Preston and Prof. A. Wilson for Aβ40 16-22. The UK 850 MHz solid-state NMR Facility was funded by EPSRC, BBSRC, and the University of Warwick, including funding through Birmingham Science City Advanced Materials Projects 1 and 2, supported by Advantage West Midlands and the European Regional Development Fund.

■ REFERENCES

(1) (a) Hard, T.; Lendel, C. *J. Mol. Biol.* **2012**, *421*, 441. (b) Amijee, H.; Madine, J.; Middleton, D. A.; Doig, A. J. *Biochem. Soc. Trans.* **2009**, *37*, 692.

(2) Lu, J.-X.; Qiang, W.; Yau, W.-M.; Schwieters, C. D.; Meredith, S. C.; Tycko, R. *Cell* **2013**, *154*, 1257.

(3) van Horssen, J.; Wesseling, P.; van den Heuvel, L.; de Waal, R. M. W.; Verbeek, M. M. *Lancet Neurol.* **2003**, *2*, 482.

(4) (a) Abedini, A.; Raleigh, D. P. *Org. Lett.* **2005**, *7*, 693. (b) Castillo, G. M.; Lukito, W.; Ngo, C.; Snow, A. D. *Brain Pathol.* **1997**, *7*, 1369. (c) Castillo, G. M.; Lukito, W.; Wight, T. N.; Snow, A. D. *J. Neurochem.* **1999**, *72*, 1681.

(5) Valle-Delgado, J. J.; Alfonso-Prieto, M.; de Groot, N. S.; Ventura, S.; Samitier, J.; Rovira, C.; Fernandez-Busquets, X. *FASEB J.* **2010**, *24*, 4250. (b) Guptabansal, R.; Frederickson, R. C. A.; Brunden, K. R. *J. Biol. Chem.* **1995**, *270*, 18666.

(6) Karran, E.; Mercken, M.; De Strooper, B. *Nat. Rev. Drug Discovery* **2011**, *10*, 698.

(7) Meneghetti, M. C. Z.; Hughes, A. J.; Rudd, T. R.; Nader, H. B.; Powell, A. K.; Yates, E. A.; Lima, M. A. *J. R. Soc., Interface* **2015**, *12*, 20150589.

(8) Madine, J.; Pandya, M. J.; Hicks, M. R.; Rodger, A.; Yates, E. A.; Radford, S. E.; Middleton, D. A. *Angew. Chem., Int. Ed.* **2012**, *51*, 13140.

(9) Lindahl, B.; Eriksson, L.; Lindahl, U. *Biochem. J.* **1995**, *306*, 177.

(10) (a) Paravastu, A. K.; Leapman, R. D.; Yau, W. M.; Tycko, R. *Proc. Natl. Acad. Sci. U.S.A.* **2008**, *105*, 18349. (b) Petkova, A. T.; Leapman, R. D.; Guo, Z. H.; Yau, W. M.; Mattson, M. P.; Tycko, R. *Science* **2005**, *307*, 262.

(11) Colvin, M. T.; Silvers, R.; Frohm, B.; Su, Y.; Linse, S.; Griffin, R. G. *J. Am. Chem. Soc.* **2015**, *137*, 7509.

(12) Zulueta, M. M. L.; Lin, S.-Y.; Lin, Y.-T.; Huang, C.-J.; Wang, C.-C.; Ku, C.-C.; Shi, Z.; Chyan, C.-L.; Irene, D.; Lim, L.-H.; Tsai, T.-I.; Hu, Y.-P.; Arco, S. D.; Wong, C.-H.; Hung, S.-C. *J. Am. Chem. Soc.* **2012**, *134*, 8988.

(13) Yates, E. A.; Santini, F.; Guerrini, M.; Naggi, A.; Torri, G.; Casu, B. *Carbohydr. Res.* **1996**, *294*, 15.

(14) Patching, S. G.; Henderson, P. J. F.; Sharples, D. J.; Middleton, D. A. *Mol. Membr. Biol.* **2013**, *30*, 129.

(15) Elena, B.; Lesage, A.; Steuernagel, S.; Bockmann, A.; Emsley, L. *J. Am. Chem. Soc.* **2005**, *127*, 17296.

(16) (a) Portieri, A.; Harris, R. K.; Fletton, R. A.; Lancaster, R. W.; Threlfall, T. L. *Magn. Reson. Chem.* **2004**, *42*, 313. (b) Timonen, J. T.; Pohjala, E.; Nikander, H.; Pakkanen, T. T. *Pharm. Res.* **1998**, *15*, 110.

(17) Liang, J. M.; Ma, Y.; Chen, B.; Munson, E. J.; Davis, H. T.; Binder, D.; Chang, H. T.; Abbas, S.; Hsu, F. L. *J. Phys. Chem. B* **2001**, *105*, 9653.

(18) Platzer, G.; Okon, M.; McIntosh, L. P. *J. Biomol. NMR* **2014**, *60*, 109.

(19) Jaroniec, C. P.; Tounge, B. A.; Herzfeld, J.; Griffin, R. G. *J. Am. Chem. Soc.* **2001**, *123*, 3507.

(20) Sarkar, A.; Desai, U. R. *PLoS One* **2015**, *10*, 0141127.

DOI: 10.1021/jacs.6b02816
J. Am. Chem. Soc. 2016, 138, 8328−8331